RESEARCH ARTICLE

Comparison of model-specific histopathology in mouse models of COVID-19

Sidi Yang[1] | Liu Cao[1] | Wenting Xu[2] | Tiefeng Xu[1] | Birong Zheng[1] |
Yanxi Ji[1] | Siyao Huang[1] | Lihong Liu[1] | Jie Du[1] | Hong Peng[1] |
Huan Zhang[3] | Jingdiao Chen[3] | Bixia Ke[3] | Huanying Zheng[3] |
Xiaoling Deng[3] | Chunmei Li[1] | Deyin Guo[1]

[1]Centre for Infection and Immunity Studies (CIIS), School of Medicine, Shenzhen Campus of Sun Yat-sen University, Guangdong, Shenzhen, China

[2]Department of Pathology, The International Peace Maternity & Child Health Hospital of China Welfare Institute (IPMCH), Shanghai Jiao Tong University, Shanghai, China

[3]Center for Disease Control and Prevention of Guangdong Province, Guangzhou, Guangdong, China

Correspondence
Deyin Guo, Centre for Infection and Immunity Studies (CIIS), School of Medicine, Shenzhen Campus of Sun Yat-sen University, Shenzhen 518107, Guangdong, China.
Email: guodeyin@mail.sysu.edu.cn

Abstract

A novel coronavirus, severe acute respiratory syndrome coronavirus 2 (SARS-CoV-2), has been identified as the causative agent of the current coronavirus disease 2019 pandemic. Development of animal models that parallel the clinical and pathologic features of disease are highly essential to understanding the pathogenesis of SARS-CoV-2 infection and the development of therapeutics and prophylactics. Several mouse models that express the human angiotensin converting enzyme 2 (hACE2) have been created, including transgenic and knock-in strains, and viral vector-mediated delivery of hACE2. However, the comparative pathology of these mouse models infected with SARS-CoV-2 are unknown. Here, we perform systematic comparisons of the mouse models including K18-hACE2 mice, KI-hACE2 mice, Ad5-hACE2 mice and CAG-hACE2 mice, which revealed differences in the distribution of lesions and the characteristics of pneumonia induced. Based on these observations, the hACE2 mouse models meet different needs of SARS-CoV-2 researches. The similarities or differences among the model-specific pathologies may help in better understanding the pathogenic process of SARS-CoV-2 infection and aiding in the development of effective medications and prophylactic treatments for SARS-CoV-2.

KEYWORDS
SARS-CoV-2, pneumonia, histopathology, mouse models, ACE2

1 | INTRODUCTION

The coronavirus disease 2019 (COVID-19) pandemic, caused by severe acute respiratory syndrome coronavirus 2 (SARS-CoV-2), has rapidly spread throughout the world. Although Molnupiravir and Paxlovid were granted emergency use authorization by the US Food and Drug Administration for the treatment of COVID-19, the clinical therapeutic effect remains to be further observed.[1,2] At present, it is still a high priority for research community to improve our understanding of the SARS-CoV-2 infection and

---

Sidi Yang and Liu Cao contributed equally to this work.

pathogenesis, and to develop new therapies and preventative treatments against COVID-19. One major approach in achieving these goals has been large-scale screening in preclinical small animal models, particularly mice. As with SARS-CoV, SARS-CoV-2 enter host cells via the interaction of the viral Spike (S) protein with human angiotensin converting enzyme 2 (hACE2).[3] Unfortunately, mouse ortholog of ACE2 is incompatible with SARS-CoV-2 S protein, and therefore, typical wild-type mouse strains are not susceptible to SARS-CoV-2. Overcoming this limitation requires either mouse adaptation of the virus, or heterologous expression of hACE2 in mice.

Several mouse models that express the hACE2 gene were created including transgenic and knock-in strains, as well as viral vector-mediated delivery of hACE2. Transgenic models include hACE2 expression under the control of the human cytokeratin (K18) epithelial cell promoter (K18-hACE2), or the synthetic CAG composite promoter (CAG-hACE2) driving high levels of expression in eukaryotic cells.[4,5] The knock-in model was generated by knocking-in hACE2 (KI-hACE2) into endogenous mouse *Ace2* loci.[6] The vector-mediated delivery of hACE2 has been successfully established, which adopts a recombinant human adenovirus type 5-expressing hACE2 (Ad5-hACE2) under the CMV promoter.[7] Although the hACE2 mice as described above fully support SARS-CoV-2 replication, the pathogenesis does not accurately model the disease course seen in humans.[8] Therefore, choosing a suitable mouse model which can replicate the human disease, or some aspects thereof, as closely as possible, is more befitting to us to understand the pathogenesis of SARS-CoV-2 infection.

Histopathology has initially been and is still being used today to diagnose infections in humans or animals.[9] It has been a powerful, reliable, and reproducible tool to better understand disease pathogenesis and evaluate novel treatments of the current virus outbreaks.[10] In addition to qualitative diagnoses, semi-quantitative assessment of lesions for histopathology are a common approach to assess all preclinical models used for the development of novel treatment strategies and acceptance by regulatory agencies.[11,12] Previous studies have revealed that the most pathological changes caused by SARS-CoV-2 were interstitial pneumonia in different hACE2 mice.[4,6,13,14] However, pathological description for SARS-CoV-2 murine pneumonia existing to date are very superficial, addressing only a few, rather unspecific parameters. More importantly, they hardly allow for a differentiating perspective between distinct types of hACE2 mice. Hence, there is an urgent need for more precise and model-specific parameters to allow for an accurate description and semi-quantitative evaluation of lung alterations in hACE2 mice. Here, we systematically describe and compare the histopathological changes at acute stage of the four types of SARS-CoV-2 infection hACE2 mouse models which include K18-hACE2 mice, KI-hACE2 mice, Ad5-hACE2 mice and CAG-hACE2 mice.

2 | MATERIALS AND METHODS

2.1 | Viral strains

The KI-hACE2 mice were infected with SARS-CoV-2 (B.1, hCoV-19/CHN/SYSU-IHV/2020 strain, Accession ID on GISAID: EPI_ISL_444969) which was isolated from a sputum sample of a woman admitted to the Eighth People's Hospital of Guangzhou. Other hACE2 mice models were infected with SARS-CoV-2 (B.1.617.2, GDPCC 2.00096) which was isolated from a patient infected with SARS-CoV-2 Delta variant admitted in the Guangzhou Eighth People's Hospital by Center for Disease Control and Prevention of Guangdong Province.

2.2 | Mice

B6.Cg-Tg(K18-human ACE2)2Prlmn/J (Jax strain 000664, K18-hACE2) mice were purchased from the Jackson Laboratory. The hACE2 knock-in mice (KI-hACE2) were provided by the National Institutes for Food and Drug Control, Beijing, China. C57BL/6-Tgtn (CAG-hACE2-IRES-Luciferase-WPRE-polyA) Smoc (CAG-hACE2) were purchased from Shanghai Model Organisms Institute, China. Ad5-hACE2 mice were established as previously described.[14] Mice were provided with sterile water and chow ad libitum and acclimatized for at least 1 week before experimental manipulation.

2.3 | Viral infections

The Biosafety Committee of Sun Yat-sen University approved work with infectious SARS-CoV-2 virus strains under BSL3 conditions. All sample inactivation was performed according to Biosafety Committee of Sun Yat-sen University approved standard operating procedures for removal of specimens from high containment. All in vivo studies were performed in accordance with the animal experiment protocol approved by the Institutional Animal Care and Use Committee of Sun Yat-sen University. All mice were maintained in a specific pathogen-free animal facility at Sun Yat-sen University.

Female transgenic K18-hACE2 mice were inoculated intranasally (i.n.) with 50 μl sterile Dulbecco's modified Eagle medium (DMEM) containing 10^4 PFU SARS-CoV-2 (B.1.617.2). At 3 days postinfection (dpi), mice were euthanized, and lung tissues were collected for hematoxylin and eosin (H&E) staining. Female KI-hACE2 mice were i.n. with 50 μl sterile DMEM containing 2×10^5 PFU SARS-CoV-2 (B.1). At 4 dpi, mice were euthanized, and lung tissues were collected for H&E staining. Female CAG-hACE2 mice were i.n. with 50 μl sterile DMEM containing 5×10^3 PFU SARS-CoV-2 (B.1.617.2). At 3 dpi, mice were euthanized, and lung tissues were collected for H&E staining. For in vivo delivery of Ad5 vectors to the lung, female C57BL/6 mice were housed in a BSL-2 facility for intranasal

TABLE 1   The comparison of outcomes of the hACE2 mouse models to SARS-CoV-2 infection

	K18-hACE2	KI-hACE2	Ad5-hACE2	CAG-hACE2
Promoter	Human K18 promoter	Mouse ACE2 promoter	CMV promoter	CAG promoter
Viral strains	B.1.617.2	B.1	B.1.617.2	B.1.617.2
Infections dose	1×10^4 PFU	2×10^5 PFU	1×10^5 PFU	5×10^3 PFU
Route of infection	Transnasal	Transnasal	Transnasal	Transnasal
Mortality (%)	100	0	0	100
Weight loss	Yes	No	Yes	Yes
Survival days (p.i.)	5–7	n.a.	n.a.	2–5

Abbreviations: hACE2, human angiotensin converting enzyme 2; SARS-CoV-2, severe acute respiratory syndrome coronavirus 2.

instillation of 2.5×10^8 FFU of Ad5-ACE2 vectors. Five days posttransduction transferred to a BSL-3 facility for challenge with 10^5 PFU SARS-CoV-2 (B.1.617.2). At 2 dpi, mice were euthanized, and lung tissues were collected for H&E staining.

2.4 | Histopathology

The lung tissues were processed through routine histologic methods. In brief, the lung tissues were fixed in 10% neutral buffered formalin for 24 h at room temperature, embedded in paraffin, and cut into 4-μm thick sections. The sections were then subjected to H&E staining to show lesions. All photomicrographs were automatically digitized using the Aperio CS2 slide scanner (Leica Biosystems Imaging Inc.) and image files were generated using the NDP.view2 Viewing software.

The evenly distributed whole-organ horizontal sections throughout the entire lungs were microscopically evaluated to assess the distribution and character of pathologic alterations: −, absent, within normal limits; +, minor, approximately 25%–50% or less of corresponding pathological changes are observed; ++, major, over 50% of corresponding pathological changes are noted. All examinations were performed by trained veterinary experimental pathologists.

3 | RESULTS

3.1 | Establishment mouse models of SARS-CoV-2 infection

All hACE2 mouse models used in this study were inoculated i.n. with different doses of SARS-CoV-2 and monitored for body weight loss and survival. Briefly, K18-hACE2 transgenic mice were infected with 10^4 PFU of SARS-CoV-2 B.1.617.2 strain (Delta variant), which showed progressive weight loss and all died within 7 days. The KI-hACE2 mice were infected with 2×10^5 PFU of SARS-CoV-2 (B.1 strain), but significant weight loss was not observed. In contrast, Ad5-hACE2 transduced C57BL/6 mice infected with 10^5 PFU SARS-CoV-2 (B.1.617.2 strain) showed weight loss from day 3 on,

and body weight gradually returned after day 6, but these mice did not die by SARS-CoV-2 infection. With 5×10^3 PFU SARS-CoV-2 (B.1.617.2 strain) challenge, CAG-hACE2 mice uniformly started losing weight at 3 days postinoculation, and all died within 5 days (Table 1).

3.2 | Pathological features of K18-hACE2 mice with SARS-CoV-2 infection

K18-hACE2 mice, also known as B6.Cg-Tg (K18-ACE2) 2Prlmn/J, were first generated by McCray and colleagues in 2007.[15] hACE2 expression in K18-hACE2 mice is driven by human cytokeratin gene promoter that is active in the airway epithelial cells.[15] Recent research indicates that intranasal inoculation with SARS-CoV-2 caused the development of pneumonia, which is consistent with our results.[4] Here, we evaluated the lung histopathological changes at 3 dpi (Figure 1A). All SARS-CoV-2-infected mice exhibited multifocal, interstitial pneumonia (Figure 1B) with marked type II pneumocyte hyperplasia, peribranchial, alveolar and perivascular inflammation comprised of mainly lymphocytes, macrophages, and neutrophils. Increased vascular permeability was associated with moderate alveolar and perivascular edema (Figure 1C–E). Most vascular walls had marked fibrinoid degeneration (Figure 1F) and consecutive vascular thrombosis (Figure 1G) as well as vasculitis. Moreover, pronounced hemorrhage within alveolar spaces, and interstitial, and prominent perivascular lymphocytic cuffing was a characteristic change (Figure 1H). A moderate necrosis of bronchial epithelial cell was observed whereas no alveolar wall necrosis was present. The histopathology of lung tissue showed that the alveolar structure of the K18-hACE2 control group was intact (Figure 1I)

3.3 | Pathological features of KI-hACE2 mice with SARS-CoV-2 infection

The KI-hACE2 mice, which was generated by CRISPR/Cas9 knock-in technology by replacing the endogenous mouse ACE2 (mACE2) with the human ACE2.[6] H&E staining showed that mouse lungs displayed a diffusely distributed interstitial pneumonia at 4 dpi with SARS-CoV-
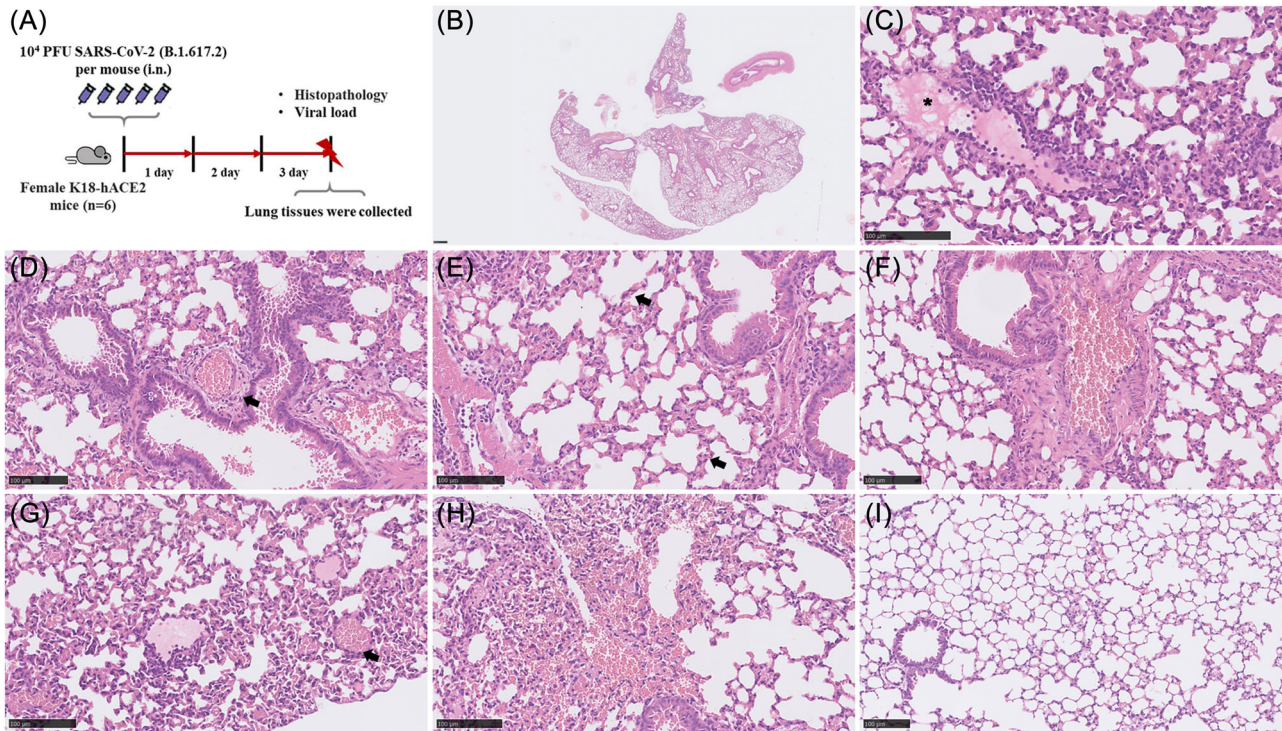
FIGURE 1 K18-hACE2 mice infection with SARS-CoV-2. Schematic of the experiment of viral infection in K18-hACE2 mice (A). At 3 dpi, the viral titer in the lungs of the infected K18-hACE2 mice ($n = 6$) was 5.15×10^5 copies/µl on the average and lung histology of mice exhibit multifocal interstitial pneumonia (B) with moderate alveolar (C, asterisk) and perivascular edema (D, arrowhead), marked type II pneumocyte hyperplasia (E, arrowhead) and fibrinoid degeneration of blood vessels (F), vascular thrombosis (G, arrowhead) and hemorrhage (H). (I) as a lung histology of control mice. (B–I) Representative images are shown. Bar (B), 500 µm; (C–I), 100 µm. hACE2, human angiotensin converting enzyme 2; SARS-CoV-2, severe acute respiratory syndrome coronavirus 2
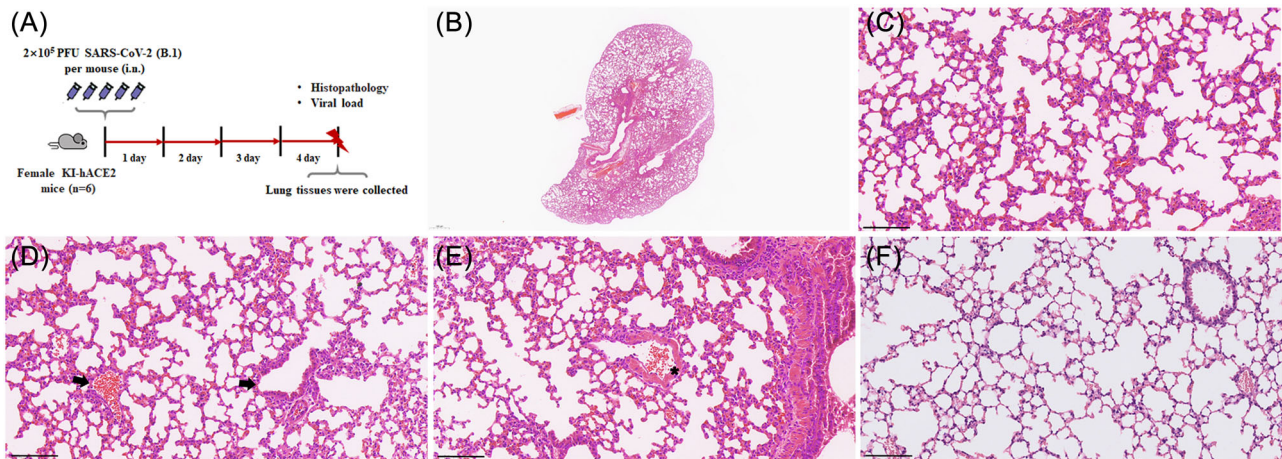
FIGURE 2 KI-hACE2 mice infection with SARS-CoV-2. Schematic of the experiment of viral infection in KI-hACE2 mice (A). At 4 dpi, the viral titer in the lungs of the infected KI-hACE2 mice ($n = 6$) was 3.92×10^4 copies/µl on the average and lung histology of mice exhibit in diffuse (B), mixed-cellular interstitial pneumonia (C) with bronchial epithelial cells and alveolar wall were moderately necrotic (D, arrowhead), mild to moderate fibrinoid degeneration of blood vessels (E, asterisk) and hemorrhage. (F) as a lung histology of control mice. (B–F) Representative images are shown. Bar (B), 500 µm; (C–F), 100 µm. dpi, days postinfection; hACE2, human angiotensin converting enzyme 2; SARS-CoV-2, severe acute respiratory syndrome coronavirus 2

2 (Figure 2A-C). The character of pneumonia included moderate infiltration of lymphocytes, macrophages, and neutrophils into peribranchial, alveolar and perivascular space whereas no lymphocytic perivascular cuffing was present . Compared to the K18-hACE2 transgenic model mentioned above, bronchial epithelial cells and alveolar wall were moderately necrotic (Figure 2D). Furthermore, vascular walls had mild to moderate fibrinoid degeneration and areas of hemorrhage within alveoli and interstitial (Figure 2E). Neither

alveolar edema nor perivascular edema were present. The histopathology of lung tissue showed that the alveolar structure of the KI-hACE2 control group was intact (Figure 2F).

3.4 | Pathological features of Ad5-hACE2 mice with SARS-CoV-2 infection

We used adenovirus constructs to transduce C57BL/6 mice by intranasal inoculation of 2.5×10^8 FFU of Ad5-ACE2. Five days posttransduction, mice were infected with SARS-CoV-2. At 2 dpi, examination of lung tissues from mice demonstrated in multifocally extensive interstitial pneumonia but predominantly located near the lung hilus (Figure 3A). Similar to K18-hACE2 transgenic model, the peribranchial, alveolar and perivascular areas were predominantly infiltrated by lymphocytes, macrophages, and neutrophils. Unlike K18-hACE2 model, perivascular edema and vascular thrombosis was hardly observed, but protein-rich alveolar edema (Figure 3D) was present albeit to a lesser extent. Here, prominent perivascular lymphocytic cuffing, vasculitis as well as alveolar wall necrosis were observed (Figure 3E). Bronchial epithelial cells were moderately necrotic (Figure 3F), and type II alveolar epithelial cells were moderately hyperplasia. Furthermore, a small portion of venous

blood vessels had fibrinoid degeneration (Figure 3G) and, albeit to a much lesser extent, areas of hemorrhage within alveoli and interstitium were present. Figure 3H as a lung histology of Ad5-hACE2 control mice.

3.5 | Pathological features of CAG-hACE2 mice with SARS-CoV-2 infection

In parallel, we used an advanced newly developed hACE2-transgenic C57BL/6 mouse model CAG-hACE2-IRES-Luc-Tg, which express hACE2 under the CAG promoter at high levels of gene expression.[16] To further evaluate the lung histopathological changes, mice were euthanized at 3 dpi, and lung tissues were collected to H&E staining (Figure 4A). Histologically, mice lungs displayed a diffusely distributed interstitial pneumonia (Figure 4B) and compare with the peribranchial and intra-alveolar areas, the perivascular areas had obvious inflammation which were predominantly infiltrated by lymphocytes and fewer neutrophils and macrophages (Figure 4C) whereas only mild lymphocytic perivascular cuffing (Figure 4D). A moderate necrosis of bronchial epithelial cell (Figure 4E), whereas no alveolar wall necrosis was present. Similar to KI-hACE2 model mentioned above, neither alveolar edema nor perivascular edema were present as well as type II
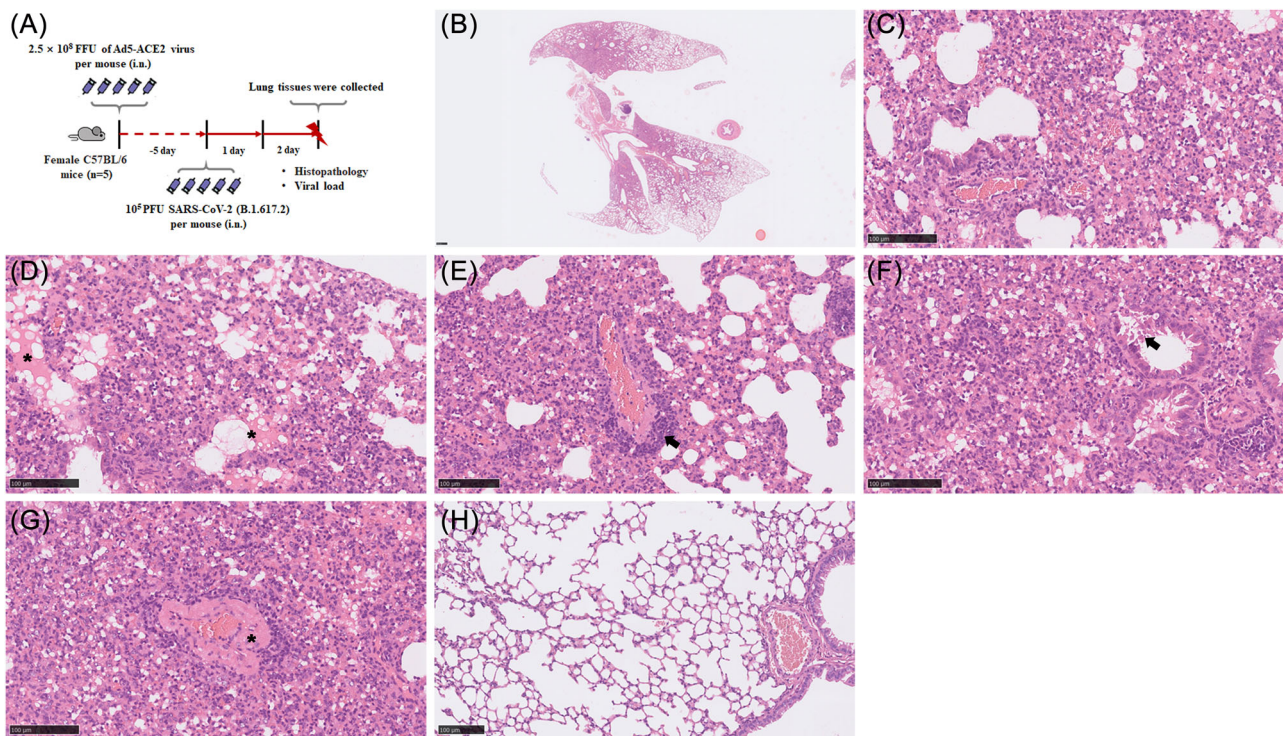
FIGURE 3 Ad5-hACE2 mice infection with SARS-CoV-2. Schematic of the experiment of viral infection in Ad5-hACE2 mice (A). At 2 dpi, and the viral titer in the lungs of the infected Ad5-hACE2 mice (n = 5) was 1.17×10^6 PFU/g on the average and lung histology of mice resulted in extensive, predominantly located near the lung hilus (B), mixed-cellular interstitial pneumonia (C) with protein-rich alveolar edema (D, asterisk), prominent lymphocytic perivascular cuffing (E, arrowhead), alveolar walls and moderately bronchial epithelial cells necrotic (F, arrowhead) and moderate fibrinoid degeneration of blood vessels (G, asterisk). (H) as a lung histology of control mice. (B–H) Representative images are shown. Bar (B), 500 μm; (C–H), 100 μm. dpi, days postinfection; hACE2, human angiotensin converting enzyme 2; SARS-CoV-2, severe acute respiratory syndrome coronavirus 2
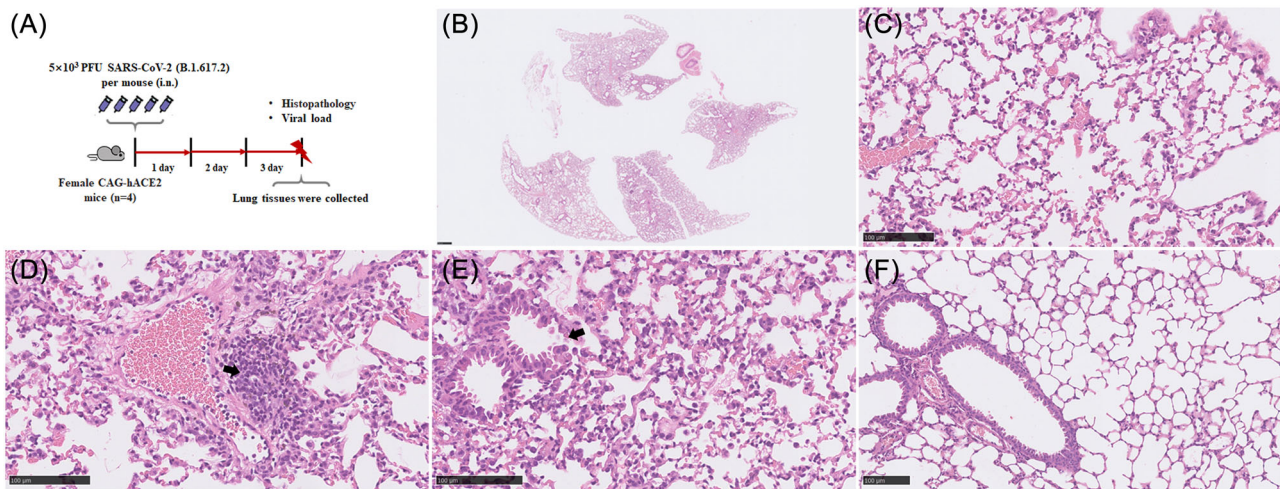
FIGURE 4 CAG-hACE2 mice infection with SARS-CoV-2. Schematic of the experiment of viral infection in CAG-hACE2 mice (A). At 3 dpi and the viral titer in the lungs of the infected CAG-hACE2 mice (*n* = 4) was 2.09 × 10³ copies/µl on the average and lung histology of mice developed a diffusely distributed interstitial pneumonia (B), predominantly infiltrated by lymphocytes and fewer neutrophils and macrophages (C), mild lymphocytic perivascular cuffing (D, arrowhead) and moderate necrosis of bronchial epithelial cell (E, arrowhead). (F) as a lung histology of control mice. (B–F) Representative images are shown. Bar (B), 500 µm; (C–F), 100 µm. dpi, days postinfection; hACE2, human angiotensin converting enzyme 2; SARS-CoV-2, severe acute respiratory syndrome coronavirus 2

alveolar epithelial cells were moderately hyperplasia. Furthermore, vasculitis and areas of hemorrhage within alveoli and interstitial were occasionally present. Figure 4F as a lung histology of CAG-hACE2 control mice.

4 | DISCUSSION

In the present study, we provide a detailed descriptive overview of histopathological features at acute stage of SARS-CoV-2 infection in four hACE2 mouse models. The models employed in this study were well established, which had been repeatedly confirmed in our previous works and also successfully used in previous studies from other laboratories.[4,6,13,14,17,18] Our model-specific description parameters (Table 2) are helpful to distinguish histopathological features of different hACE2 mouse models accurately. The potential of these parameters for future evaluation of hACE2 mouse models is extensive.

Comparing the different staining in the four hACE2 mouse models, varying degrees of inflammation, especially interstitial pneumonia, and varying degrees of lesions, including inflammatory cell infiltration, pulmonary edema, hemorrhaging, necrosis of the bronchial epithelial cells, and hyperplasia of type II alveolar epithelial cells were observed. In the lungs of K18-hACE2 mice, exudative pathological changes were found, exhibiting pulmonary edema, inflammatory cell infiltration, hemorrhaging, fibrinous exudates and perivascular lymphocytic cuffing, suggesting acute pneumonia. This is in consistence with the previous study that have also reported that K18-hACE2 mice exhibited potentially lethal disease.[19] Additionally, we found that the prominent inflammatory cells in the CAG-hACE2 mice was different. In our study, the diffuse infiltration of numerous

lymphocytes and fewer neutrophils and macrophages were observed in the perivascular, peribranchial and intraalveolar space of CAG-hACE2 mice. However, three other models exhibit peribranchial, alveolar and perivascular inflammation comprised of mainly lymphocytes, macrophages, and neutrophils. In contrast, in the lungs of CAG-hACE2 mice, diffuse and focal lymphocyte infiltration occurred in the perivascular and mildly in the peribranchial and intraalveolar space. These differences in inflammatory cell infiltration suggest that inflammatory cells may function in the development of SARS-CoV-2 infection. Similar to other study, the KI-hACE2 mice challenged with SARS-CoV-2 developed mild interstitial pneumonia characterized by moderate infiltration of inflammatory cells, alveolar septal thickening, and limited pathology was observed.[6,20]

When the distributions of lesions were compared among the four models tested, two distinct patterns could be distinguished. Unlike the other models' lungs that displayed a diffusely distribution, the lesions of Ad5-hACE2 mice were focused around central airways and blood vessels close to the lung hilus with the periphery less or not affected, which can likely be explained by the method used for delivery of Ad5 viral vector. When acute mouse pneumonia is sampled for molecular studies such as mRNA or protein quantitation, the uneven and often quite asymmetrical distributions have a tremendous impact in practical terms. As we know, K18 transgenic mice expressing human ACE2 is driven by a cytokeratin promoter in the airway epithelial cells, KI-hACE2 mice that express hACE2 under an endogenous promoter in place of murine ACE2, CAG-hACE2 mice expressing hACE2 under the control of the synthetic CAG composite promoter driving high levels of expression in eukaryotic cells and Ad5-hACE2 mice restricted hACE2 expression in the respiratory tract.[7] Thus, the cellular expression of hACE2 varies in different mouse models and such difference may lead to differing levels of viral

TABLE 2 Model-specific pathological changes in mouse models of SARS-CoV-2 infection

Evaluation criteria	K18-hACE2	KI-hACE2	Ad5-hACE2	CAG-hACE2
Peribranchial inflammation	+	+	++	+
Perivascular inflammation	++	+	++	++
Interstitial inflammation	++	+	++	+
Intraalveolar inflammation	++	+	++	+
Bronchial epithelial cell necrosis	+	+	+	+
Alveolar wall necrosis	−	+	++	−
Infiltration by neutrophils	++	+	++	+
Infiltration by macrophages	++	+	++	+
Infiltration by lymphocytes	++	+	++	++
Alveolar edema	+	−	+	−
Perivascular edema	+	−	−	−
Perivascular lymphocytic cuffing	++	−	++	+
Hyperplasia of type II alveolar epithelial cells	++	+	+	+
Vasculitis	++	−	++	+
Fibrinoid degeneration ofvascular walls	++	+	+	−
Vascular thrombosis	+	−	−	−
Hemorrhage (interstitial, intraalveolar)	++	+	+	+

Note: -, absent; +, minor; ++, major.

Abbreviations: hACE2, human angiotensin converting enzyme 2; SARS-CoV-2, severe acute respiratory syndrome coronavirus 2.

replication in different cell types, different histopathological features in lung tissues and differences in disease pathogenesis.

Fatal human cases of SARS-CoV-2 infection are histologically characterized by diffuse alveolar damage with intra-alveolar hyaline membranes, edema, denuding of bronchiolar epithelia, fibrin deposits, vascular thrombosis, type II pneumocyte hyperplasia and lymphocyte infiltration.[21–23] These findings provide evidence for the pathological features of SARS-CoV-2, which is in common with other similar respiratory illnesses, such as MERS-CoV.[24] Despite the analyses of the pathological responses observed within the lungs of the SARS-CoV-2-infected hACE2 mice resemble those observed in human COVID-19 patients with regard to the lesions and cell tropism, no mouse model fully recapitulates all aspects of COVID-19, and the continued development of models is necessary to address the diverse spectrum of pathophysiology encompassed by SARS-CoV-2 infection.

In summary, different mouse models, including the transgenic hACE2 mice and non-genetically engineered mouse model allowing researchers to mimic the different outcomes and features of SARS-CoV-2 infection in humans, from asymptomatic to severe multiorgan disease. Our histological results showed that the lung lesions in Ad5-hACE2 mice were relatively not distributed homogeneously, which only partially simulated the pathology of COVID-19 and could be useful in screening antivirals or testing vaccines. In the acute stage of the disease, the pathological damage of KI-hACE2 mouse lungs was relatively mild. Considering that the no clinical symptoms or mortality was observed in this model, the hACE2 knock-in model may be more

useful in elucidating disease mechanisms. In contrast, although the acute phase of COVID-19 can be well simulated by the CAG-hACE2 mouse model, the lung injury is not typical from the histopathology of the CAG-hACE2 mice, suggesting that this model may be useful in testing vaccines and antivirals. However, the K18-hACE2 model developed edema-associated acute lung injury (ALI) and best recapitulates the histopathological changes of COVID-19, including the acute and severe pathological process, indicating that this model could be suitable for testing of SARS-CoV-2 countermeasures such as immune-modulatory interventions and antiviral. Thus, the hACE2 mouse models can meet different needs of SARS-CoV-2 researches and suitable mouse model can be selected depending on the purpose of the study. Although it is one-sided to evaluate the suitability of different models only from histopathology, this method is to some extent a key means of evaluating preclinical models.

In conclusion, we established animal models of SARS-CoV-2 infection using K18-hACE2 mice, KI-hACE2 mice, Ad5-hACE2 mice and CAG-hACE2 mice. We have uncovered a model-specific lung lesion with characteristic histopathology, which provides a framework that may help in better understanding the pathogenic process of SARS-CoV-2 infection and aiding in the development of effective medications and prophylactic treatments for SARS-CoV-2.

AUTHOR CONTRIBUTIONS

Deyin Guo: conceived and planned the overall structure of the article. **Sidi Yang and Liu Cao:** contributed to development of methodology

CONFLICTS OF INTEREST

The authors declare no conflicts of interest.

DATA AVAILABILITY STATEMENT

The data that support the findings of this study are available from the corresponding author upon reasonable request.

ORCID

Deyin Guo http://orcid.org/0000-0002-8297-0814

REFERENCES

1. (2021) Coronavirus (COVID-19) Update: FDA Authorizes First Oral Antiviral for Treatment of COVID-19.
2. (2021) Coronavirus (COVID-19) Update: FDA Authorizes Additional Oral Antiviral for Treatment of COVID-19 in Certain Adults.
3. Hoffmann M, Kleine-Weber H, Schroeder S, et al. SARS-CoV-2 cell entry depends on ACE2 and TMPRSS2 and is blocked by a clinically proven protease inhibitor. *Cell*. 2020;181: 271-280 e278.
4. Oladunni FS, Park JG, Pino PA, et al. Lethality of SARS-CoV-2 infection in K18 human angiotensin-converting enzyme 2 transgenic mice. *Nat Commun*. 2020;11:6122.
5. Tseng CT, Huang C, Newman P, et al. Severe acute respiratory syndrome coronavirus infection of mice transgenic for the human Angiotensin-converting enzyme 2 virus receptor. *J Virol*. 2007;81: 1162-1173.
6. Sun SH, Chen Q, Gu HJ, et al. A mouse model of SARS-CoV-2 infection and pathogenesis. *Cell Host Microbe*. 2020;28: 124-133 e124.
7. Gurumurthy CB, Quadros RM, Richardson GP, Poluektova LY, Mansour SL, Ohtsuka M. Genetically modified mouse models to help fight COVID-19. *Nat Protoc*. 2020;15:3777-3787.
8. Dinnon KH, 3rd, Leist SR, Schafer A, et al. A mouse-adapted model of SARS-CoV-2 to test COVID-19 countermeasures. *Nature*. 2020; 586:560-566.
9. Klopfleisch R. Multiparametric and semiquantitative scoring systems for the evaluation of mouse model histopathology—a systematic review. *BMC Vet Res*. 2013;9:123.
10. Matute-Bello G, Downey G, Moore BB, et al, Acute Lung Injury in Animals Study, G. An official American Thoracic Society workshop report: features and measurements of experimental acute lung injury in animals. *Am J Respir Cell Mol Biol*. 2011;44:725-738.
11. West MA, Roman A, Sayan E, et al. A minimum core outcome dataset for the reporting of preclinical chemotherapeutic drug studies: lessons learned from multiple discordant methodologies in the setting of colorectal cancer. *Crit Rev Oncol Hematol*. 2017;112:80-102.
12. Dietert K, Gutbier B, Wienhold SM, et al. Spectrum of pathogen- and model-specific histopathologies in mouse models of acute pneumonia. *PLoS One*. 2017;12:e0188251.
13. Jiang RD, Liu MQ, Chen Y, et al. Pathogenesis of SARS-CoV-2 in transgenic mice expressing human angiotensin-converting enzyme 2. *Cell*. 2020;182:50-58 e58.
14. Sun J, Zhuang Z, Zheng J, et al. Generation of a broadly useful model for COVID-19 pathogenesis, vaccination, and treatment. *Cell*. 2020; 182:734-743 e735.
15. McCray PB, Jr., Pewe L, Wohlford-Lenane C, et al. Lethal infection of K18-hACE2 mice infected with severe acute respiratory syndrome coronavirus. *J Virol*. 2007;81:813-821.
16. Tgtn(CAG-hACE2-IRES-Luciferase). NM-TG-200002.
17. Cao Liu, L. Y, Yang Sidi, et al. The adenosine analogue prodrug ATV006 is orally bioavailable and has potent preclinical efficacy against SARS-CoV-2 and its variants. *bioRxiv*. 2021
18. Xia S, Lan Q, Zhu Y, et al. Structural and functional basis for pan-CoV fusion inhibitors against SARS-CoV-2 and its variants with preclinical evaluation. *Signal Transduct Target Ther*. 2021;6:288.
19. Yinda CK, Port JR, Bushmaker T, et al. K18-hACE2 mice develop respiratory disease resembling severe COVID-19. *PLoS pathogens*. 17, 2021:e1009195.
20. Winkler ES, Chen RE, Alam F, et al. SARS-CoV-2 causes lung infection without severe disease in human ACE2 knock-in mice. *J Virol*. 2021:JVI0151121.
21. Martines RB, Ritter JM, Matkovic E, et al. Pathology and pathogenesis of SARS-CoV-2 associated with fatal coronavirus disease, United States. *Emerging Infect Dis*. 2020;26:2005-2015.
22. Yao XH, Luo T, Shi Y, et al. A cohort autopsy study defines COVID-19 systemic pathogenesis. *Cell Res*. 2021;31:836-846.
23. Hariri LP, North CM, Shih AR, et al. Lung histopathology in coronavirus disease 2019 as compared with severe acute respiratory sydrome and H1N1 influenza: a systematic review. *Chest*. 2021;159:73-84.
24. Yu P, Xu Y, Deng W, et al. Comparative pathology of rhesus macaque and common marmoset animal models with Middle East respiratory syndrome coronavirus. *PLoS One*. 2017;12:e0172093.

How to cite this article: Yang S, Cao L, Xu W, et al. Comparison of model-specific histopathology in mouse models of COVID-19. *J Med Virol*. 2022;94:3605-3612. doi:10.1002/jmv.27747